Int. J. Solids Structures Vol. 23, No. 6, pp. 751–767, 1987
Printed in Great Britain.
0020-7683/87 $3.00+.00

ANALYSIS OF A STRAIN SOFTENING CONSTITUTIVE MODEL

G. FRANTZISKONIS and C. S. DESAI
Department of Civil Engineering and Engineering Mechanics, University of Arizona, Tucson, AZ 85721, U.S.A.

(*Received* 4 *December* 1985; *in revised form* 10 *July* 1986)

Abstract—The paper first examines the question of uniqueness of a basic yet simplified constitutive model with strain softening. It is shown that the constitutive equations lead to a unique solution for the case of rate-dependent as well as rate-independent formulation and its implementation in finite element analysis shows mesh size insensitivity in the hardening and softening regimes. Conditions for formation of narrow shear bands are developed and discussed. It is shown that as the damage accumulates the material approaches localization of deformation.

1. INTRODUCTION

A number of materials, such as concrete, rock and dense soils, show a decrease in strength during progressive straining after the peak strength is reached. This phenomenon is termed "strain softening". From experimental observations of strain softening, it has been found that strain softening may not be a material property of concrete, rock or soil treated as continua, but rather the performance of a structure (finite sized specimen) composed of microcracks, joints and interfaces that result in an overall loss of strength. A review and discussion on this subject is given by Sandler[1] and Read and Hegemier[2]. If strain softening is assumed to be a true (continuum) material property, various anomalous conditions may arise with respect to solution of boundary and initial value problems. As shown by Valanis[3], these anomalies can lead to loss of uniqueness in the softening part of the stress–strain response. Subsequently, loss of uniqueness leads to numerical instabilities. This is illustrated from the high sensitivity of the numerical solution to the finite element mesh size, Sandler[1], and Pietruszczak and Mroz[4].

Structural changes affect considerably the behavior of concrete and rock. The major structural changes can be identified as microcrack propagation, microcrack initiation and joining of microcrack. The laws that govern these structural changes are not fully understood. Despite this, a model could qualitatively describe the above-mentioned effects of structural changes. Such an approach is proposed by the authors and is described and implemented in Refs [5–7]. Here the behavior of a material element is decomposed in two parts[5–8], topical or continuum and damaged or stress relieved. The decomposition is enacted over the volume, V, which consists of V_t, termed the topical or continuum part, and V_0, termed the damaged part such that $V = V_t + V_0$ always. The damaged part obeys a so-called stress-relieved constitutive law, and the topical part a frictional hardening (*non-softening*) constitutive law. Although both the decomposed parts or fractions are *non-softening*, with accumulation of damage, the overall response is softening after a peak value is reached. On this basis, a damage variable is defined which subsequently leads to a definition of a second-order tensor that describes the overall structural changes. The formation and growth of damage is responsible for strain softening, degradation of elastic shear modulus and induced anisotropy. The model has shown good agreement between predictions and experimental observations for a concrete, a rock and a soil.

Details of the model and verification of laboratory behavior for a number of materials are presented in Refs [5–7]; here the major attention is given to mathematical analysis of the model for two factors: (1) uniqueness and sensitivity of solution to (finite element) mesh size, and (2) the effect of damage growth on formation of localized deformation in terms of a bifurcation point leading to non-uniform deformations. The uniqueness analysis is based on the work of Valanis[3] and considers small deformations. Concepts proposed

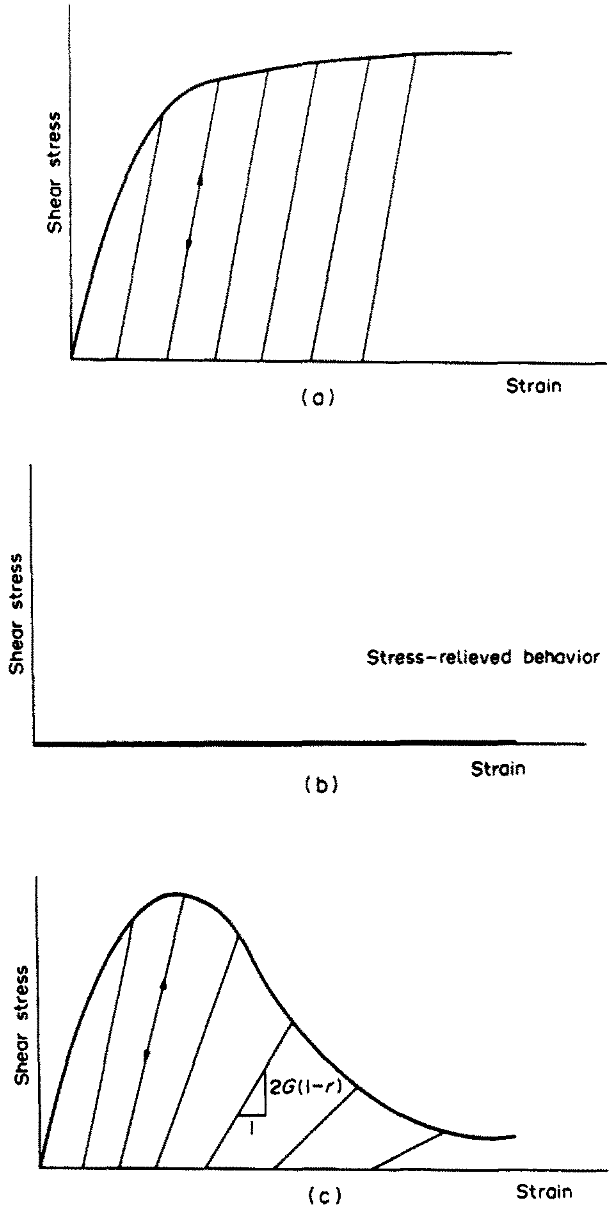

Fig. 1. Schematic of decomposition of material behavior: (a) topical, elastic–plastic part; (b) damaged part; (c) average behavior.

and used in Refs [9–15] are employed for analysis of localization of deformation which involves finite deformations. Because the two studies are based on small and large deformations, they are described in two separate parts. First a brief review of the proposed model is presented, however.

2. CONSTITUTIVE RELATIONS FOR THE MODEL

The following brief description of the model is adopted from Refs [5–7]. As already mentioned, the material behavior is decomposed in two parts or fractions; the topical part and the stress-relieved or damaged part. The corresponding volumes on which the two parts act are denoted as V_t and V_0. Accordingly, σ^t_{ij} and σ^d_{ij} denote the topical and the damaged stress tensors, respectively. As schematically shown in Fig. 1, the topical part is assumed to obey an elastic–plastic constitutive law, while the damaged part has zero shear resistance. The damaged constitutive relation may be termed as rigid perfectly plastic with zero yield strength. The ratio $r = V_0/V$ is defined ($0 \leq r \leq 1$) with the interpretation that before any load is applied, $r = 0$ and when the residual stress level is reached, r reaches an ultimate value denoted as r_u which tends to 1. Let σ_{ij} denote the average or mean stress tensor. Following physical reasoning as well as experimental observations, a relation between r, σ_{ij} and σ^t_{ij} is established as

$$\sigma_{ij} = (1 - r)\sigma^t_{ij} + \frac{r}{3}\sigma^t_{kk}\delta_{ij} \tag{1}$$

and δ_{ij} is the Kronecker delta. For compatibility at the continuum level, the strains ε_{ij} in the two parts are considered to be equal.

The elastoplastic constitutive relations for the topical part are written as

$$\dot{\sigma}^t_{ij} = C^{e\text{-}p}_{ijkl}\dot{\varepsilon}_{kl} \tag{2a}$$

for loading, and as

$$\dot{\sigma}^t_{ij} = C^{e}_{ijkl}\dot{\varepsilon}_{kl} \tag{2b}$$

for elastic unloading. In eqns (2), an overdot indicates time rate, $C^{e\text{-}p}_{ijkl}$ is the elastoplastic constitutive tensor corresponding to a specified yield surface and hardening rule, C^e_{ijkl} is the elasticity tensor; elasticity is assumed linear and isotropic. This means that unloading is isotropic and loading anisotropic, and this is an assumed simplification of the reality.

It is noted here that since the topical behavior is non-softening, $C^{e\text{-}p}_{ijkl}$ is always positive definite. As shown subsequently, this property is of importance when uniqueness is considered. It follows from eqns (1) and (2) that

$$\dot{\sigma}_{ij} = (1 - r)C^e_{ijkl}\dot{\varepsilon}_{kl} + \frac{r}{3}\delta_{ij}C^{e\text{-}p}_{ppkl}\dot{\varepsilon}_{kl} - \dot{r}S^t_{ij} \tag{3a}$$

for loading, and

$$\dot{\sigma}_{ij} = (1 - r)C^e_{ijkl}\dot{\varepsilon}_{kl} + \frac{r}{3}\delta_{ij}C^{e}_{ppkl}\dot{\varepsilon}_{kl} \tag{3b}$$

for unloading. In eqns (3) tensor S^t_{ij} is the deviatoric part of σ^t_{ij}. As it can be seen from eqns (3b) and (1), it is assumed that no damage is induced during unloading. Also, elastic, and thus unloading, properties degrade as damage progresses. This property is depicted through eqn (3b) and is schematically shown in Fig. 1(c). Induced anisotropy, an obvious property of cracked media, is captured through the last term in eqn (3a).

In order that the formulation is complete, an evolution law for the variable r is defined, and is expressed in terms of internal variable such as trajectory of deviatoric plastic strains and its rate as

$$\dot{r} = f(\xi_D, \dot{\xi}_D) \tag{4}$$

where $\dot{\xi}_D = (\dot{E}^p_{ij}\dot{E}^p_{ij})^{1/2}$ and the superscript p denotes plastic strain, and $\dot{E}^p_{ij}$ is the deviator tensor of $\dot{\varepsilon}^p_{ij}$. In Ref. [5] the following evolution for r was proposed:

$$r = r_u - r_u \exp(-\kappa\xi^R_D) \tag{5}$$

where r_u, κ, and R are positive dimensionless material constants. In more general terms, eqn (5) can be written as

$$\dot{r} = U\dot{\xi}_D \tag{6}$$

where $U = U(\xi_D)$ is always positive, representing the slope of the r vs ξ_D curve. Now, the question of uniqueness is examined. It is shown that different types of evolution laws for r introduce different types of formulation.

3. UNIQUENESS

In a recent publication by Valanis[3], the question of uniqueness of solution of initial value problems in softening materials is examined. An inequality is established which is true for all materials, irrespective of their constitution. It is shown that a number of constitutive equations that give rise to realistic softening behavior lead to a unique solution. Ordinarily rate-dependent models lead to a unique solution but rate-independent ones either fail to lead to a unique solution or the question of uniqueness is difficult to analyze. Valanis addresses a simple uniaxial model (eqn (6.6) in Ref. [3]) which assures uniqueness only when the model is formulated as rate dependent. It seems that formulation of a rate-independent model that assures uniqueness in the softening regime is not trivial.

For convenient reference, we will provide here a brief outline of the results in Ref. [3]. Let the solution be unique at time t, and let Δt be a vanishingly small non-zero time interval. Let two solutions exist at $t + \Delta t$. Let $\dot{\sigma}^1_{ij}$, $\dot{\varepsilon}^1_{ij}$, and $\dot{\sigma}^2_{ij}$, $\dot{\varepsilon}^2_{ij}$ be the stress and strain rates corresponding to the two solutions evaluated at t. If Δ denotes the difference between the two solutions, e.g. $\Delta\dot{\varepsilon}_{ij} = \dot{\varepsilon}^2_{ij} - \dot{\varepsilon}^1_{ij}$, then the solution is unique if

$$\Delta\dot{\sigma}_{ij}\Delta\dot{\varepsilon}_{ij} > 0. \tag{7}$$

Now, we examine the conditions under which the constitutive equations represented through eqns (3) and (4) provide a unique solution. Assuming two solutions, we obtain from eqn (3)

$$(\dot{\sigma}_{ij})^2 = L_{ijkl}\dot{\varepsilon}^2_{kl} - \dot{r}^2 S^t_{ij} \tag{8a}$$

$$(\dot{\sigma}_{ij})^1 = L_{ijkl}\dot{\varepsilon}^1_{kl} - \dot{r}^1 S^t_{ij} \tag{8b}$$

where

$$L_{ijkl} = (1 - r)C^{e\text{-}p}_{ijkl} + \frac{r}{3}C^{e\text{-}p}_{ppkl}\delta_{ij} \tag{9}$$

and superscripts 1 and 2 denote the two solutions.

Now we consider two special cases of eqn (4)

Case 1

$$\dot{r} = \dot{r}(\xi_D); \tag{10}$$

Case 2

$$\dot{r} = \dot{r}(\xi_D, \dot{\xi}_D) \tag{11}$$

such that eqn (6) holds for eqn (11). We note that Case 1 expressed by eqn (10) brings a rate dependency in the formulation, while Case 2 expressed by eqn (11) or eqn (6) represents a rate-independent problem. If eqn (5) is used, the formulation is rate independent. Here the question of uniqueness for both cases is considered.

Case 1

It follows from eqns (8) and (10) that

$$\Delta\dot{\sigma}_{ij}\Delta\dot{\varepsilon}_{ij} = \Delta\dot{\varepsilon}_{ij}L_{ijkl}\Delta\dot{\varepsilon}_{kl}. \tag{12}$$

As already mentioned, $C^{e\text{-}p}_{ijkl}$ is always positive definite. Then since $0 \leqslant r \leqslant 1$, it follows from eqn (9) that L_{ijkl} is always positive definite. Then the right-hand side of eqn (12) is positive; thus eqn (7) is satisfied. Thus we see that the rate-dependent formulation satisfies the uniqueness criterion.

Case 2

It follows from eqns (8) and (6) that

$$\Delta\dot{\sigma}_{ij}\Delta\dot{\varepsilon}_{ij} = \Delta\dot{\varepsilon}_{ij}L_{ijkl}\Delta\dot{\varepsilon}_{kl} - \Delta\dot{r}\Delta\dot{\varepsilon}_{ij}S^{\mathrm{i}}_{ij} \tag{13}$$

where $\Delta\dot{r} = \dot{r}^2 - \dot{r}^1$.

From eqn (6) we obtain

$$\Delta\dot{r} = U\Delta\dot{\xi}_{\mathrm{D}} \tag{14}$$

and from the definition of $\dot{\xi}_{\mathrm{D}}$, we have

$$\Delta\dot{\xi}_{\mathrm{D}} = \alpha_{ij}\Delta\dot{E}^{\mathrm{p}}_{ij} \tag{15a}$$

$$\alpha_{ij} = \dot{E}^{\mathrm{p}}_{ij}(\dot{E}^{\mathrm{p}}_{kl}\dot{E}^{\mathrm{p}}_{kl})^{-1/2}. \tag{15b}$$

Since $\Delta\dot{E}^{\mathrm{p}}_{ij} = \Delta\dot{\varepsilon}^{\mathrm{p}}_{ij} - \frac{1}{3}\Delta\dot{\varepsilon}^{\mathrm{p}}_{nn}\delta_{ij}$ and $\Delta\dot{\varepsilon}^{\mathrm{p}}_{ij} = \Delta\dot{\varepsilon}_{ij} - \Delta\dot{\varepsilon}^{\mathrm{e}}_{ij}$, we have

$$\Delta\dot{E}^{\mathrm{p}}_{ij} = (\Delta\dot{\varepsilon}_{st} - \Delta\dot{\varepsilon}^{\mathrm{e}}_{st})\left(\delta_{is}\delta_{jt} - \frac{1}{3}\delta_{st}\delta_{ij}\right) \tag{16}$$

where superscript e denotes elastic.

The elastic strain rates are related to $\dot{\sigma}^{\mathrm{i}}_{ij}$, so that

$$\dot{\varepsilon}^{\mathrm{e}}_{st} = D^{\mathrm{e}}_{stkl}\dot{\sigma}^{\mathrm{i}}_{kl} \tag{17a}$$

$$D^{\mathrm{e}}_{stkl} = \frac{1}{2G}\delta_{sk}\delta_{lt} - \frac{K}{2G(2G+3K)}\delta_{kl}\delta_{st} \tag{17b}$$

where G, K denote the initial elastic shear and bulk moduli, respectively. It follows from eqns (2a) and (14)–(17) that

$$\Delta\dot{r} = UT_{pq}\Delta\dot{\varepsilon}_{pq} \tag{18a}$$

where

$$T_{pq} = \alpha_{pq} - \alpha_{st}D^{\mathrm{e}}_{stkl}C^{e\text{-}p}_{klpq}. \tag{18b}$$

Now the elastoplastic tensor $C^{e\text{-}p}_{ijkl}$ needs to be written explicitly. In Ref. [5] a generalized plasticity model[6] was used where the associative flow rule was assumed. Following Mandel[9] and Rudnicki and Rice[10], $C^{e\text{-}p}_{ijkl}$ is written in terms of the internal friction coefficient, μ, and the dilatancy factor, β. If $\beta \neq \mu$, the non-associative rule holds. Since here it is not required that $\beta = \mu$, the associative flow rule assumption is not necessary.

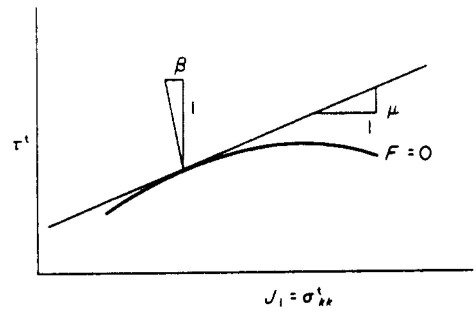

Fig. 2. Geometric interpretation of μ and β.

The geometric interpretation of β and μ[9, 10] is shown schematically in Fig. 2. For clarity, in the Appendix, β and μ are related to the generalized model used herein, and the strain rates are expressed in terms of the stress rates. If h denotes the plastic modulus and

$$\tau^t = \left(\frac{1}{2}S^t_{ij}S^t_{ij}\right)^{1/2}$$

the elastoplasic constitutive tensor is expressed as

$$C^{e\text{-}p}_{abpq} = G(\delta_{pa}\delta_{qb} + \delta_{bp}\delta_{aq}) + \left(K - \frac{2}{3}G\right)\delta_{ab}\delta_{pq}$$

$$- \frac{\left(\frac{G}{\tau^t}S^t_{ab} + \beta K\delta_{ab}\right)\left(\frac{G}{\tau^t}S^t_{pq} + K\mu\delta_{pq}\right)}{h + G + \mu K\beta} \tag{19}$$

which is the inverse relation of eqn (A6). Now from eqn (1), we obtain that $S_{ij} = (1 - r)S^t_{ij}$, thus

$$\frac{S_{ij}}{\tau} = \frac{S^t_{ij}}{\tau^t} \tag{20}$$

where

$$\tau = \left(\frac{1}{2}S_{ij}S_{ij}\right)^{1/2}.$$

The topical stress in eqn (19) can be eliminated by using eqn (20), thus, from now on the mean stress will appear in place of the topical stress in eqn (19).

As it is seen from eqn (15b), α_{ij} is a unit vector in the direction of $\dot{E}^p_{ij}$ in the six-dimensional space. It is a property of the plasticity theory, and it can be seen from eqn (A6) that $\dot{E}^p_{ij}$ is proportional to S^t_{ij}. Then the following holds:

$$\alpha_{ij} = \frac{S^t_{ij}}{\tau^t\sqrt{2}} \tag{21}$$

and from eqn (20)

$$\alpha_{ij} = \frac{S_{ij}}{\tau\sqrt{2}}. \tag{22}$$

From eqns (18b), (17b), (19), (20) and (22), it follows that

$$T_{pq} = \frac{\frac{G}{\tau}S_{pq} + K\mu\delta_{pq}}{(h + G + \mu K\beta)\sqrt{2}}. \tag{23}$$

From eqns (1), (5), (18a) and (23), we obtain

$$\Delta\dot{r}\Delta\dot{\varepsilon}_{ij}S^{\text{t}}_{ij} = T_1 + T_2 \tag{24a}$$

$$T_1 = \frac{U}{\sqrt{2}}\frac{\frac{G}{\tau}S_{kl}}{(h + G + \mu K\beta)}\frac{S_{ij}}{(1 - r)}\Delta\dot{\varepsilon}_{ij}\Delta\dot{\varepsilon}_{kl} \tag{24b}$$

$$T_2 = \frac{U}{\sqrt{2}}\frac{K\mu\sigma_{kl}}{(h + G + \mu K\beta)}\frac{S_{ij}}{(1 - r)}\Delta\dot{\varepsilon}_{ij}\Delta\dot{\varepsilon}_{kl}. \tag{24c}$$

Equation (24a) defines the second term on the right-hand side of eqn (13). Since L_{ijkl} is always positive definite, the first term in eqn (13) is always positive. In order that the solution be unique, it is sufficient to show that the absolute value of the second term in eqn (13) is smaller than the first term. As shown subsequently, the absolute value of the second term is not only less but much smaller than the first term in eqn (13). From eqns (9), (19) and (20), L_{ijkl} is expressed as

$$L_{abpq} = (1 - r)G(\delta_{pa}\delta_{qb} + \delta_{bp}\delta_{aq}) + \left[K - \frac{2}{3}(1 - r)G\right]\delta_{ab}\delta_{pq} - \frac{\left[\frac{(1 - r)G}{\tau}S_{ab} + \beta K\delta_{ab}\right]\left[\frac{(1 - r)G}{\tau}S_{pq} + K(1 - r)\mu\delta_{pq}\right]}{(1 - r)(h + G + \mu K\beta)}. \tag{25}$$

We note that eqn (25) may be obtained from eqn (19) by making the following substitutions:

$$G \to G' = (1 - r)G \tag{26a}$$

$$\mu \to \mu' = (1 - r)\mu \tag{26b}$$

$$h \to h' = (1 - r)h. \tag{26c}$$

From eqn (25) it follows that

$$\Delta\dot{\varepsilon}_{ij}\Delta\dot{\varepsilon}_{kl}L_{ijkl} = T'_1 + T'_2 + T_3 \tag{27a}$$

$$T'_1 = (1 - r)\frac{\left(\frac{G}{\tau}\right)^2 S_{kl}}{(h + G + \mu K\beta)}S_{ij}\Delta\dot{\varepsilon}_{ij}\Delta\dot{\varepsilon}_{kl} \tag{27b}$$

$$T'_2 = (1 - r)\frac{\frac{G}{\tau}K\mu\delta_{kl}}{(h + G + \mu K\beta)}S_{ij}\Delta\dot{\varepsilon}_{ij}\Delta\dot{\varepsilon}_{kl} \tag{27c}$$

$$T_3 = \Delta\dot{\varepsilon}_{ij}\Delta\dot{\varepsilon}_{kl}L_{ijkl} - T'_1 - T'_2. \tag{27d}$$

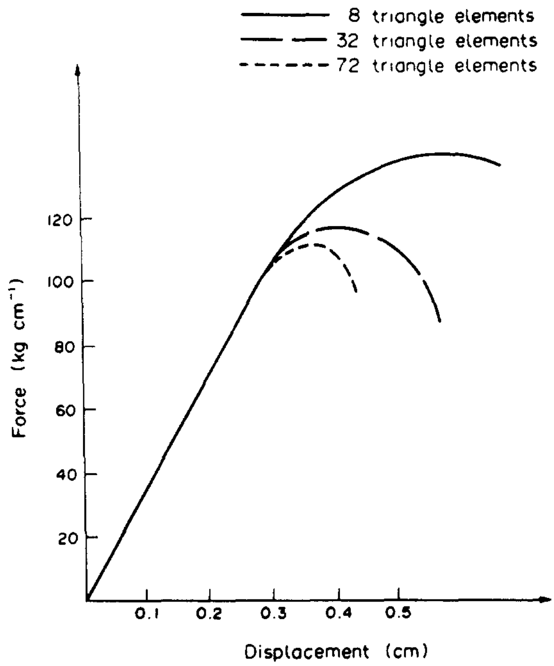

Fig. 3. Typical load–displacement relationship resulting from analysis termed as standard (after Ref. [4]).

From eqns (24) and (27), we obtain

$$\frac{T_1}{T_1'} = \frac{T_2}{T_2'} = \frac{U}{\sqrt{2}}\frac{\tau^{\mathrm{t}}}{G'}. \tag{28}$$

Relations (24), (27) and (28) imply that a sufficient condition for eqn (7) to hold is

$$\frac{U}{\sqrt{2}}\frac{\tau^{\mathrm{t}}}{G'} < 1. \tag{29}$$

From eqns (5) and (6) it follows that U is a dimensionless (positive) number representing the slope of the r vs ξ_D curve[5]. Its value depends on the value of ξ_D and the constants associated with the damage evolution law. In order to estimate the order of its magnitude, the values of the constants estimated for a concrete[5–7] are employed. The values of these constants will vary from material to material and it is reasonable to assume that the order of the values may not be much different for similar materials. Then since ξ_D is of the order of deviatoric plastic strain and τ^{t}/G' is of the order of deviatoric elastic strains (much less than unity), the value of the left-hand side of eqn (29) is found to vary between zero and order of 10^{-2}, thus, eqn (29) is satisfied. Equation (29), derived from eqn (7) implies that uniqueness is satisfied conditionally. Although it provides uniqueness for a number of stress paths considered herein, further research may be needed for a general proof. Additional use of the bifurcation theories based on large deformations (see subsequent sections) may be appropriate for such general analyses.

4. NUMERICAL IMPLEMENTATION

As mentioned in the Introduction, when strain softening of materials is treated as an elasticity or elastoplasticity problem, numerical analysis may suffer from instabilities and high sensitivity to mesh size. The subject is discussed in detail in Refs [1, 4]. Typical load–displacement relationships showing effect of mesh sizes for a different constitutive model, as reported in Ref. [4], are shown in Fig. 3. Details of the problem are given later (Fig. 4).

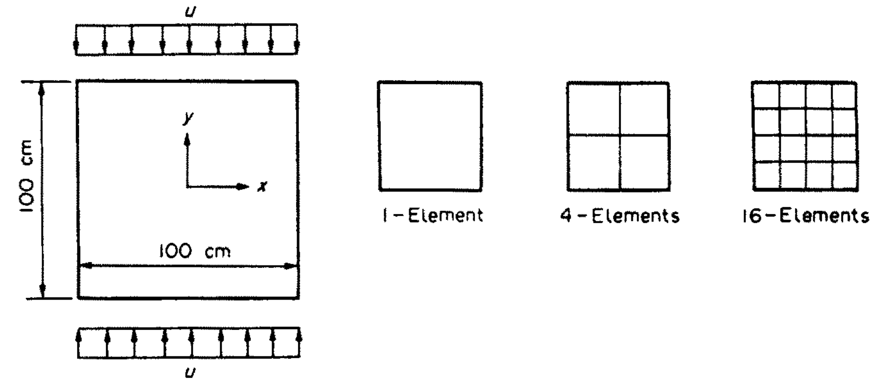

Fig. 4. Finite element discretization for example problem.

As discussed in Ref. [3], lack of uniqueness in the softening regime may be the reason for such mesh sensitivities when the standard procedures are employed.

In Ref. [7] the procedure for numerical implementation of the damage constitutive model has been discussed. The principle of virtual work leads to the following incremental equations in matrix notation[16]:

$$\int_V \mathbf{B}^{\mathrm{T}}\, \mathrm{d}\boldsymbol{\sigma}\, \mathrm{d}V = \mathrm{d}\mathbf{Q} \tag{30}$$

where $\mathbf{B}$ is the strain–displacement transformation matrix, $\mathrm{d}\boldsymbol{\sigma}$ denotes increment in stress, $\mathrm{d}\mathbf{Q}$ is the increment in external force including surface and body forces, and superscript T denotes transpose. The incremental form of the stress–strain relation is written as

$$\mathrm{d}\boldsymbol{\sigma} = \mathbf{L}\, \mathrm{d}\boldsymbol{\varepsilon} - \mathrm{d}r\, \mathbf{S}^{t} \tag{31}$$

where the expression for $\mathbf{L}$ is given in eqn (9), $\mathrm{d}r$ denotes the increment of r, and $\mathbf{S}^{t}$ is the topical stress vector. From eqns (30), (31) and the incremental strain–displacement relations, we obtain

$$\mathbf{k}\, \mathrm{d}\mathbf{q} = \mathrm{d}\mathbf{Q} + \mathrm{d}\mathbf{Q}^{r} \tag{32a}$$

where

$$\mathbf{k} = \int_V \mathbf{B}^{\mathrm{T}}\mathbf{L}\mathbf{B}\, \mathrm{d}V \tag{32b}$$

and

$$\Delta\mathbf{Q}^{r} = \int_V \mathbf{B}^{\mathrm{T}}\, \mathrm{d}r\, \mathbf{S}^{t}\, \mathrm{d}V. \tag{32c}$$

In eqns (32), $\mathbf{k}$ is always positive definite since $\mathbf{L}$ is always positive definite. Thus, $\mathbf{k}$ in eqns (32) is non-softening and problems related to negative modulus are avoided. Further, $\Delta\mathbf{Q}^{r}$, termed the "damage force", is responsible for the softening in the average constitutive description. Thus, the formulation is such that the stiffness matrix always remains positive definite. The decomposition, depicted schematically in Fig. 1, and discussed previously, involves the damage force that modifies positive definite $\mathbf{k}$, thus giving the capability of stable calculations in the softening regime.

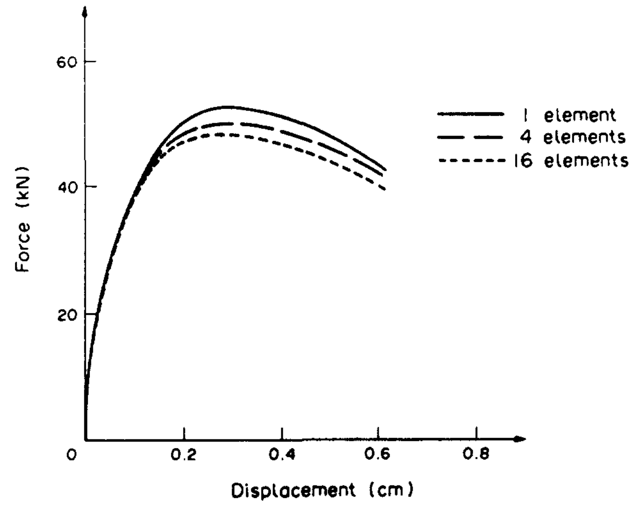

Fig. 5. Computed load displacement curves for 1-, 4-, and 16-eight-noded quadrilateral elements.

4.1. *Mesh sensitivity*

For illustration purposes, the following problem adopted from Ref. [4] is considered. Figure 4 shows the dimensions and finite element mesh. Three different meshes were used with 1, 4 and 16 elements; the 8-noded isoparametric element is used[17]. The problem is idealized as two-dimensional and plain strain conditions are assumed.

Increments of vertical displacements were applied along the top and bottom surfaces while the horizontal displacements at the top and bottom were restrained; this represents a sticking friction condition. An iterative (Newton–Raphson) procedure[16–18] was employed for the incremental solution of the problem[7]. The material parameters are given in Ref. [5]. These material parameters were determined from multiaxial tests of a concrete[19].

Figure 5 shows the computed load–displacement curves obtained by using the model proposed herein. It is seen that the mesh-size sensitivity is insignificant as compared to the sensitivity depicted in Fig. 3 that was reported by Pietruszczak and Mroz[4]. Note that the element used in Ref. [4] was triangular with linear displacement field, whereas the element used herein is quadrilateral with quadratic displacement field. The small differences can be due to normal finite element discretization errors.

5. LOCALIZATION

Here, the possibility that the proposed damage model leads to a bifurcation point, at which nonuniform deformation can be incipient in a planar band, usually called "shear band", is examined. The condition for the localization of the deformation into a shear band can be derived from the requirement that the internal and external stress vectors across a shear band boundary are in equilibrium. This type of analysis is usually called "shear band analysis" and has been explained in detail in various publications[11–13]; such analysis and results for geomaterials are given by Rudnicki and Rice[10] and Vardoulakis[14]. A brief outline of shear band analysis based on Ref. [10] is presented here.

Let Δ denote the difference between the local field at a point in the band and the uniform field outside the band. Let the constitutive equations be written in the form

$$\overset{\nabla}{\sigma}_{ij} = E_{ijkl} D_{kl} \tag{33}$$

where $\overset{\nabla}{\sigma}_{ij}$ is the Jaumann (co-rotational) stress rate defined as

$$\overset{\nabla}{\sigma}_{ij} = \dot{\sigma}_{ij} - \sigma_{ip} W_{pj} - \sigma_{jp} W_{pi}. \tag{34}$$

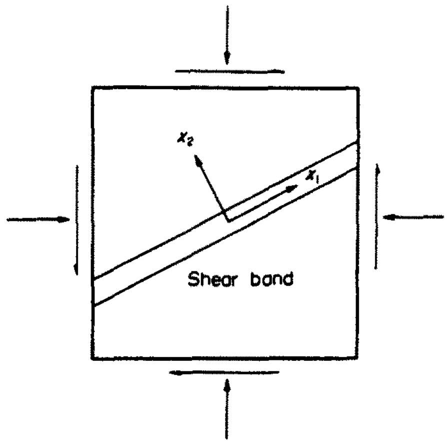

Fig. 6. Shear band and coordinate system.

In eqns (33) and (34) D_{ij} is the symmetric part, and W_{ij} the antisymmetric part of the velocity gradient, $\partial v_j/\partial x_i$, and E_{ijkl} in eqn (33) denotes the modulus tensor. Let X_i, $i = 1$, 2, 3, denote a coordinate system such that the direction X_2 is perpendicular to the shear band (Fig. 6). If, at the bifurcation of deformation rates, the values of E_{ijkl} remain the same in and outside the band[10]

$$\Delta \overset{\nabla}{\sigma}_{ij} = E_{ijkl} \Delta D_{kl}. \tag{35}$$

Expressing ΔW_{ij} and ΔD_{ij} in terms of $\Delta(\partial v_i/\partial x_j)$, the following condition for bifurcation results[10]:

$$\det |E_{2jk2} - R_{jk}| = 0 \tag{36}$$

where R_{jk} denote stress terms resulting from the expression for ΔW. If a zeroth-order analysis is to be developed, the R_{jk} terms in eqn (36) may be neglected, as compared to the E_{ijkl} terms. Such an analysis amounts to retaining the first term in an expansion of the stress/elastic modulus ratio[10].

As shown previously, eqns (3) and (9), the constitutive relations involve evolution of damage in the material. The purpose here is to examine how damage and its evolution influence the conditions for localization.

From eqns (3) and (9), the constitutive relations may be expressed as

$$\overset{\nabla}{\sigma}_{ij} = L_{ijkl} D_{kl} - \dot{r} S^1_{ij}. \tag{37}$$

From eqn (37) the following difference is formed:

$$\Delta \overset{\nabla}{\sigma}_{ij} = L_{ijkl} \Delta D_{kl} - \Delta \dot{r} S^1_{ij} \tag{38}$$

where eqn (6) holds as an evolution of the damage parameter r. In this section Δ has a different physical meaning than the one assigned in the previous section. Mathematically though, the same operations can be performed on Δ. Thus, following the same steps as in eqns (14)–(18), a relation similar to eqn (18) is obtained as

$$\Delta \dot{r} = U T_{kl} \Delta D_{kl} \tag{39}$$

and T_{kl} is expressed as in eqn (18b). From eqns (38) and (39), the following condition for localization is obtained; here the zeroth-order analysis holds:

$$\det|L_{2jk2} - UT_{k2}S^{t}_{2j}| = 0. \tag{40}$$

Following the same steps as in the previous section (relations (19)–(29)), it can be shown that the second terms on the left-hand side of eqn (40) are much smaller than the first terms as long as eqn (29) holds. Then they can be neglected. The tensor L_{ijkl} is expressed analytically through eqn (25), and the condition for localization reduces to $\det|L_{2jk2}| = 0$. As previously noted, the tensor L_{ijkl} is obtained from C^{ep}_{ijkl} by making substitutions (26). Thus, the procedure employed for bifurcation analysis of elastoplastic materials may be employed here if the following distinguishing points are considered: (1) substitutions as in eqn (26) are made, (2) the plastic modulus h, referred to the topical behavior, is always non-negative. Similar manipulations are described in Refs [10, 14]. For this reason and for compactness, we present the results for the critical value of h and the angle of inclination of the shear band. At the localization conditions, the following holds:

$$\left(\frac{h}{G}\right)_{cr} = \frac{\left[(1-r)X + \beta\frac{K}{G}\right]\left(X + \mu\frac{K}{G}\right)}{\frac{4}{3}(1-r) + \frac{K}{G}} - XN - N^2 - X^2 - \mu\frac{K}{G}\beta \tag{41a}$$

where

$$\frac{K}{G} = \frac{2(1+\nu)}{3(1-2\nu)}$$

and

$$X = \frac{[(1-r)\mu + \beta](1+\nu)}{2(1+\nu) + (1-r)(1-2\nu)} - \frac{N[2(1-r)(1-2\nu)] + (1+\nu)}{2(1+\nu) + (1-r)(1-2\nu)} \tag{41b}$$

and ν is the Poisson's ratio, $N = S_{22}/\tau$. The angle θ_0 which maximizes h, and hence defines the plane of localization is given by

$$\tan\theta_0 = \left(\frac{X - N_1}{N_3 - X}\right)^{1/2} \tag{42}$$

where $N_1 = S_{11}/\tau$ and $N_3 = S_{33}/\tau$. Figure 7 shows the orientation of the shear band with respect to the principal stress coordinate system. The angle θ_0 is the angle between the normal to the plane of localization and the σ_3 principal stress.

In order to interpret expressions (41) and (42), the values of h/G and θ_0 at localization are shown in Figs 8 and 9 and in Table 1 for different values of r. As mentioned before, h is always non-negative. Then negative values of h/G indicate that to the corresponding damage accumulation no critical value of h exists. During a monotonically increasing shear path, the value of h/G initially has a relatively large value and subsequently decreases. At the same time, r is initially zero and subsequently increases. At localization, the $(h/G)_{cr}$ lies on the curve shown in Fig. 8; e.g. point A. Prior to localization, a curve, schematically shown in Fig. 8, is followed until point A is reached. As shown in Table 1 and Fig. 8, the value of r influences considerably the critical value of h/G. Specifically, the greater the accumulation of damage, the closer the material comes to a state where localization of deformation can occur. This is expected since accumulation of damage brings the material closer to an instability or collapse. A basic conclusion is that damaged material is more

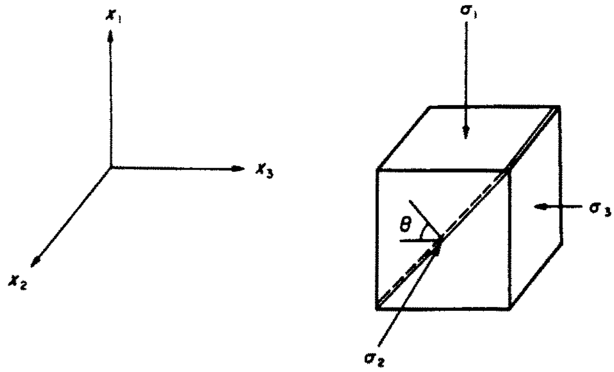

Fig. 7. Orientation of shear band in principal stress space, $\sigma_1 \geqslant \sigma_2 \geqslant \sigma_3$.

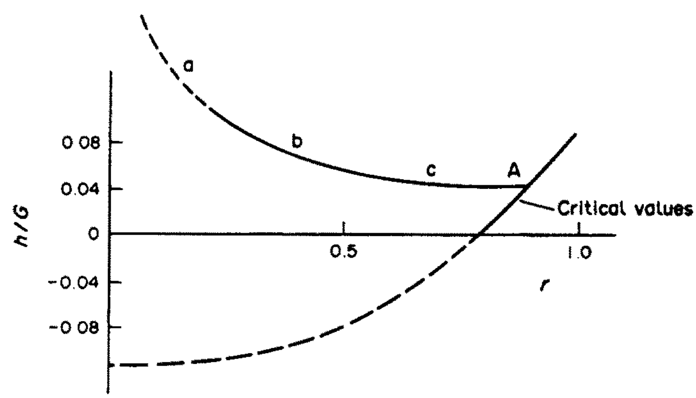

Fig. 8. Effect of damage accumulation on initiation of localization for pure shear stress condition ($N = 0$), $\mu = 0.9$, $\beta = 0.6$, $\nu = 0.3$.

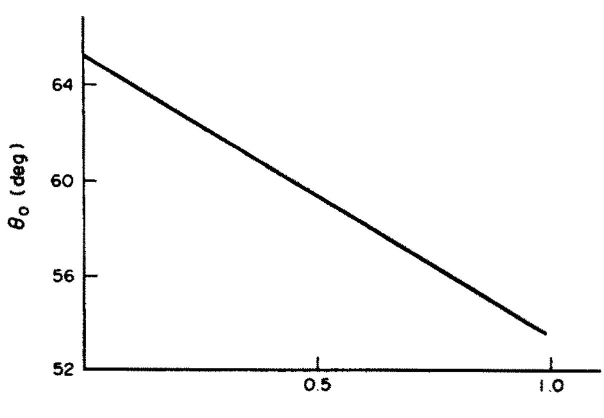

Fig. 9. Effect of damage accumulation on shear band inclination θ_0 for pure shear stress condition ($N = 0$), $\mu = 0.9$, $\beta = 0.6$, $\nu = 0.3$.

Table 1. Values of (h/G) at localization and shear band inclination angle θ_0 for various values of damage accumulation. Solution corresponds to pure shear, $N = 0$ and $\nu = 0.3$

μ	β	$(h/G)_{cr}$	θ_0 (deg.)
(a) $r = 0.5$			
0.0	0.0	0.0	45.0
0.3	0.0	0.004	46.9
0.3	0.15	−0.007	49.0
0.3	0.3	−0.009	51.0
0.6	0.0	0.016	49.0
0.6	0.15	−0.01	51.0
0.6	0.3	−0.028	53.1
0.6	0.45	−0.038	55.2
0.6	0.6	−0.04	57.4
0.9	0.0	0.036	51.0
0.9	0.15	−0.05	53.1
0.9	0.3	−0.038	55.2
0.9	0.45	−0.06	57.4
0.9	0.6	−0.08	59.6
(b) $r = 0.75$			
0.0	0.0	0.0	45.0
0.3	0.0	0.001	46.0
0.3	0.15	−0.002	48.1
0.3	0.3	0.003	50.2
0.6	0.0	0.005	47.1
0.6	0.15	−0.007	49.2
0.6	0.3	−0.009	51.3
0.6	0.45	−0.003	53.4
0.6	0.6	0.013	55.6
0.9	0.0	0.011	48.1
0.9	0.15	−0.009	50.2
0.9	0.3	−0.020	52.3
0.9	0.45	−0.022	54.5
0.9	0.6	−0.014	56.7
(c) $r = 0.9$			
0.0	0.0	0.0	45.0
0.3	0.0	0.0002	45.4
0.3	0.15	0.0018	47.5
0.3	0.3	0.014	49.7
0.6	0.0	0.0008	45.8
0.6	0.15	−0.001	47.9
0.6	0.3	0.007	50.1
0.6	0.45	0.026	52.3
0.6	0.6	0.056	54.5
0.9	0.0	0.0018	46.3
0.9	0.15	−0.0036	48.4
0.9	0.3	0.0014	50.5
0.9	0.45	0.0167	52.7
0.9	0.6	0.0426	54.9
(d) $r = 0.99$			
0.0	0.0	0.0	45.0
0.3	0.0	0.2×10^{-9}	45.0
0.3	0.15	0.0056	47.1
0.3	0.3	0.022	49.3
0.6	0.0	0.9×10^{-9}	45.0
0.6	0.15	0.0056	47.15
0.6	0.3	0.023	49.3
0.6	0.45	0.051	51.5
0.6	0.6	0.0899	53.7
0.9	0.0	0.2×10^{-8}	45.0
0.9	0.15	0.0056	47.2
0.9	0.3	0.022	49.3
0.9	0.45	0.051	51.5
0.9	0.6	0.089	53.7

inclined to instability by localization of deformation, than a material that is not damaged. The damage also affects the angle θ_0 as shown from Table 1 and Fig. 9.

Experimental measurements of conditions at the initiation of localization is not an easy task. To our knowledge, precise measurements of such conditions are not available in the literature, hence, comparisons of the theoretical predictions with observations are difficult. However, the effect of damage accumulation on the conditions under which strain localization can initiate, leading to shear band formation, have been examined here.

5.1. *Comment*

From eqns (9) and (36), it is clear that damage accumulation as well as the elastoplasticity relations, expressed through C^{ep}_{ijkl}, considerably affect the conditions for shear band formation; for instance, Molenkamp[15] found that considerable variations in the predicted instant of initiation for different elastoplastic models occurred. In this study, however, the analysis is restricted to only one elastoplastic model[5–7].

As shown in the previous section, uniqueness was associated with the constitutive relations where the theory of Valanis[3] was employed, and small deformations were considered. The localization analysis involves large deformation and shows that the formulation may allow nonuniqueness, especially at highly damaged states. The analysis suggests that initiation of localization depends on the parameters involved in the macroscopic description of damage.

6. CONCLUSIONS

The theoretical analyses for the proposed strain-softening model consisting of a topical part simulated by an isotropic hardening elastoplastic model and the fractured part simulated through a damage variable are performed for uniqueness and strain localization. It is shown that the model provides a conditional uniqueness criterion based on the method proposed by Valanis[3]. The uniqueness attribute is verified by showing that the finite element solutions for a typical problem are independent of various mesh sizes. The criterion proposed by Rudnicki and Rice[10] is used, and further, the effect of damage accumulation on the conditions under which strain localization can initiate, leading to shear band formation, is studied. It is believed that the proposed concept can provide a general yet simplified model for characterizing elastoplastic behavior of (geologic) materials undergoing microcracking and fracture leading to loss of strength and strain softening.

Acknowledgement—The research performed herein was supported through Grant No. CEE 8215344 from the National Science Foundation and Grant No. AFOSR-83-0256 from Air Force Office of Scientific Research (AFOSR). Communication and discussions with Drs H. Murakami and H. E. Read, S-CUBED, California, on the uniqueness criterion based on eqn (7) are gratefully acknowledged.

REFERENCES

1. I. S. Sandler, Strain softening for static and dynamic problems. ASME Winter Annual Meeting, Symp. on Constitutive Equations: Micro, Macro and Computational Aspects, CEQ, New Orleans (December 1984).
2. H. E. Read and G. A. Hegemier, Strain softening of rock, soil and concrete—a review article. *Mech. Mater.* 3, 271–294 (1984).
3. K. C. Valanis, On the uniqueness of solution of the initial value problem in softening materials. *J. Appl. Mech. ASME* **52**, 85-APM-29 (1985).
4. St. Pietruszczak and Z. Mroz, Finite element analysis of deformation of strain-softening materials. *Int. J. Numer. Meth. Engng* 17, 327–334 (1981)
5. G. Frantziskonis and C. S. Desai, Constitutive model with strain softening. *Int. J. Solids Structures* **23**, 733–750 (1987).
6. C. S. Desai, S. Somasundaram and G. Frantziskonis, A hierarchical approach for constitutive modelling of geologic materials. *Int. J. Numer. Analyt. Meth. Geomech.* **10** (1986).
7. G. Frantziskonis, Progressive damage and constitutive behavior of geomaterials including analysis and implementation. Doctoral dissertation, Dept. of Civil Engng and Engng Mech., University of Arizona, Tucson, Arizona (1986).
8. C. S. Desai, A consistent finite element technique for work-softening behavior. *Proc. Int. Conf. on Comp. Methods in Non-linear Mechanics* (Edited by J. T. Oden *et al.*). University of Texas, Austin, Texas (1974).
9. J. Mandel, Sur les lignes de glissement et le calcul des deplacements dans la deformation plastique. *C. r. Acad. Sci.* **225**, 1272–1273 (1947).
10. J. W. Rudnicki and J. R. Rice, Conditions for the localization of deformation in pressure-sensitive dilatant materials. *J. Mech. Phys. Solids* **23**, 371–394 (1975).
11. R. Hill, Acceleration waves in solids. *J. Mech. Phys. Solids* **10**, 1–16 (1962).
12. J. Mandel, Conditions de stabilite et postulat de Drucker. *Proc. IUTAM Symp. Rheology Soil Mech.*, Grenoble, 1964, pp. 58–68 (1966).

13. R. Hill and J. W. Hutchinson, Bifurcation phenomena in the plane tension test. *J. Mech. Phys. Solids* **23**, 239–264 (1975).
14. I. Vardoulakis, Shear band inclination and shear modulus of sand in biaxial tests. *Int. J. Numer. Analyt. Meth. Geomech.* **4**, 103–119 (1980).
15. F. Molenkamp, Comparison of frictional material models with respect to shear band initiation. *Géotechnique* **35**, 127–143 (1985).
16. C. S. Desai and J. F. Abel, *Introduction to the Finite Element Method*. Van Nostrand Reinhold, New York (1972).
17. M. M. Zaman, C. S. Desai and E. C. Drumm, Interface model for dynamic soil-structure interaction. *J. Geotech. Engng ASCE* **110**, 1257–1273 (1983).
18. B. K. Nagaraj, Modelling for interfaces and implementation. Doctoral dissertation, Dept. of Civil Engng and Engng Mech., University of Arizona, Tucson, Arizona (1986).
19. J. G. M. Van Mier, Strain softening of concrete under multiaxial loading conditions. Doctoral dissertation, Eindhoven University of Technology, The Netherlands (1984).

APPENDIX

The flow rule of associated plasticity is expressed as

$$\dot{\varepsilon}^p_{ij} = \lambda \frac{\partial F}{\partial \sigma_{ij}} \tag{A1}$$

where F is the yield surface. The coefficient λ is expressed as

$$\lambda = \frac{\dfrac{\partial F}{\partial \sigma_{ij}} C^e_{ijkl} \dot{\varepsilon}_{kl}}{\dfrac{\partial F}{\partial \sigma_{rs}} C^e_{rspq} \dfrac{\partial F}{\partial \sigma_{pq}} - H} \tag{A2}$$

where

$$H = \left(\frac{\partial F}{\partial \sigma_{kl}} \frac{\partial F}{\partial \sigma_{kl}}\right)^{1/2} \frac{\partial F}{\partial \xi}$$

and ξ is the trajectory of plastic strains equal to $\int (\dot{\varepsilon}_{ij} \dot{\varepsilon}_{ij})^{1/2}$. From eqns (A1) and (A2) we obtain

$$\lambda = \frac{1}{h'} \frac{\partial F}{\partial \sigma_{kl}} \dot{\sigma}_{kl} \tag{A3}$$

where

$$h' = -\left(\frac{\partial F}{\partial \sigma_{kl}} \frac{\partial F}{\partial \sigma_{kl}}\right)^{1/2} \frac{\partial F}{\partial \xi}.$$

Now, from the flow rule eqns (A1) and (A3), we have

$$\dot{\varepsilon}^p_{ij} = \frac{1}{h'} \frac{\partial F}{\partial \sigma_{ij}} \frac{\partial F}{\partial \sigma_{kl}} \dot{\sigma}_{kl}. \tag{A4}$$

The yield function F is expressed as

$$F = J_{2D} + \alpha J_1^n + \gamma J_1^2 = 0 \tag{A5}$$

where J_{2D} is the second invariant of the deviator stress tensor and J_1 the first invariant of the stress tensor. For convenience, only a truncated form of the general function[5, 6] is adopted herein; however, the derivation can be made for the general case also. It follows from eqns (A4) and (A5) that

$$\dot{E}_{ij} = \frac{\dot{S}_{ij}}{2G} + \frac{S_{ij}}{h'}\left[\frac{\partial F}{\partial J_1} \dot{\sigma}_{kk} + S_{kl} \dot{\sigma}_{kl}\right] \tag{A6a}$$

$$\dot{\varepsilon}_{kk} = \frac{\dot{\sigma}_{kk}}{3K} + \frac{1}{h'}\left[3\left(\frac{\partial F}{\partial J_1}\right)^2 \dot{\sigma}_{kk} + 3 \frac{\partial F}{\partial J_1} S_{kl} \dot{\sigma}_{kl}\right]. \tag{A6b}$$

From eqns (A6) and the relations involving μ and β[10], the following relations are obtained:

$$\frac{1}{h'} = \frac{1}{h}\frac{1}{4\tau^2} \tag{A7a}$$

$$\mu = \beta = \frac{3}{2}\frac{1}{\tau}\frac{\partial F}{\partial J_1}. \tag{A7b}$$

In the yield function expressed in eqn (A5), α is the hardening parameter such that $\alpha = \alpha_1/\xi^{\eta_1}$ and α_1, η_1 are the hardening constants. The constants associated with the model were evaluated for a concrete tested by Van Mier[19] and their values are given in Ref. [5].